OMAE2010-21049

ANALYSIS OF EROSION AND FAILURE IN THE SUDDEN EXPANSION FRACTURING TUBING OF DEEP GAS WELLS

Yan Xu, Zunce Wang, Sen Li, Fengxia Lv, Yuejuan Yan, Houzhen Wen
Mechanical Science and Engineering College
Daqing Petroleum Institute
Daqing, Heilongjiang, China

ABSTRACT

With the increasing of flow rate during fracturing in deep gas well, the erosion of fracturing tubing is an issue of immense concern to the industry. Based on the Euler-Euler two – fluid theory, the numerical simulations have been performed to predict the flow field in the sudden expansion fracturing tubing. The velocity distributions and sand concentration profiles are obtained, and the simulation results show that separation and reflux come into being in the sudden expansion fracturing tubing when pumping sand slurries at high rate, and the sand concentration increases at some regions. The erosion and failure of the fracturing tubing are relevant to the sand concentration, the velocity and the impact angle. The erosion model was established with the erosion experiment, and the numerical simulation results were used to describe the erosion rate of sudden expansion fracturing tubing according to the established erosion models. The mainly erosion region obtained through the simulation is basically agree with the failure region of tubing during fracturing in deep gas wells.

Key words: sudden expansion; fracturing tubing; erosion; numerical simulation

INTRODUCTION

The erosion problems encountered in deep gas well fracture involve disturbed flow at sudden expansion in fracturing tubing, where there is often flow separation accompanied by recirculation and reattachment flow. In the case of low flow, it has not attracted enough attention to the people. The erosion is more severe with increasing flow rate and sand concentration, the part of severe erosion causes tool failure, leading to fracturing failure. For example, at Song102 deep wells in Daqing Oilfield, the tubing under sudden expansion has broken at the throttle nozzle. Nine deep wells of Xujiaweizi site in Daqing Oilfield is fractured at high sand concentration and flow rate, four of which occurred to break, resulting in construction of failure.

As reported by Lotz and Heitz, high local erorsion rates can lead to substantial changes in wall geometry, which in turn modifies the structure of the flow and leads to different rates of erosion (Lotz, E. Heitz, Werkst. 1983).

The effect of changing wall geometry has been observed in industrial equipment and must be taken into account in experimental studies to determine erosion rates and in predictive models being developed to calculate erosion rate (S. Nesic, J. Postlethwaite 1991; J. Postlethwite, S. Nesic, G. Adamopoulos, D.J. Bergstrom 1992).

Oliveira studies on the axisymmetric sudden expansion pipe laminar flow with finite volume method, using numerical simulation (Oliveira P J, Pinho F T. 1997), received recirculation zone length, intensity, and position of vortex center, the results were agree well with the physical model test data. J. Postlethwaite and S. Nesic have advanced in the development of predictive models for erosion-corrosion in disturbed turbulent flows. The application of turbulence models permits the structure (velocity, pressure, turbulence fields) of the complex flow to be determined the erosion-corrosion rate (J. Postlethwaite, S. Nesic, G. Adamoroulos and D.J.Bergstrom 1993). The

application of computational fluid dynamics (CFD) to the problem of erosion in multiphase flow systems, under conditions of sudden expansion flow, can help to quantify the effects of the systems geometry on rates of erosion leading to design improvements.

In view of this practical engineering problem, the internal flow field and erosion in the absence of corrosion was studied in the sudden expansion during pumping sand slurries, adopting to the numerical simulation method. The erosion model is established, experiments were designed to determine the parameter of the erosion model, and the erosion rate is predicted.

DEEP GAS WELL PLUG FRACTURING TUBING TECHNIQUE AND EROSION OF TUBING

Fracturing tubing structure and working principle

Deep gas well plug fracturing tubing is mainly involving the reverse circulation valve, safety joints, hydraulic anchor, packer, throttling nozzle seat, sliding sleeve sandjet, plug seal section, drillable packer, movable throttling nozzle and wear joints tools, etc. The concrete structure is shown in Figure 1.

After running fracturing string, fracturing construction is operated. Firstly, the lower level is constructed, and then the ball-off and movable throttling nozzle are thrown into well, sliding sleeve sandjet is open. At this moment the sliding sleeve is sealed by the ball, throttling nozzle is sitting in its seat, and pressure drop produced as fracturing fluid flow through the throttling nozzle, make the packer set successful. The last, upper layer fracture is operated.

Erosion of tubing

The throttling nozzle is an important component of the deep gas plug fracturing tubing, shown in Figure 2, and its role in the fracturing process is to generate pressure drop in order to set the pack. As the fluid through the throttle nozzle with pumping sand amount accooumulated $100m^3$, the sudden expansion tubing under the throttle nozzle is break in Song102 deep well of Daqing oil field, the physiognomy of the failure tool after field test is shown in Figure 3.
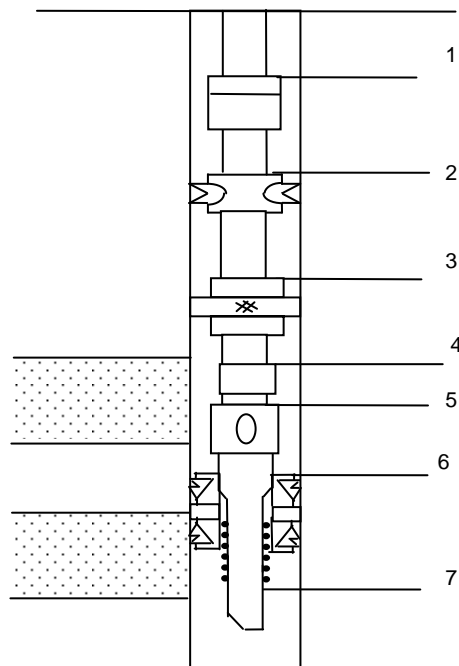

Figure 1 Deep gas well plug fracturing tubing
1. Safety joints 2. Hydraulic anchor 3. Packer 4. Throttling nozzle seat 5. Sliding sleeve sandjet   6. Drillable packer 7. Plug seal section,

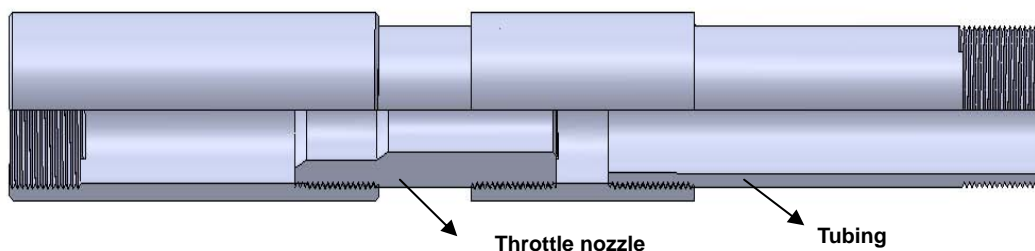**Figure 3   Erosion tubing　（Song deep 102）**

Figure 2 Fracturing tubing joint under throttle nozzle

2

Copyright © 2010 by ASME

MATHEMATIC MODEL

In this study, the fluid, including liquid phase (fracturing fluid) and solid-phase (fracturing proppant), in the fracturing process, the volume of flow rate is up to 140m³/min, the maximum volume fraction of solids is 40%, and the particle density is relatively large, two-phase is separated in the flow field. Based on Euler-Euler method, fracturing tubing solid-liquid two-phase turbulence model is established under the framework of continuum

basic assumptions：

1) the solid phase is as a continuous medium outside liquid phase as a continuous medium, a single pressure is shared by all phases, momentum and continuity equations are solved for each phase;

2) the tow-phase fluid flows is incompressible and steady turbulent;

3) solid particles can be seen as rigid and the diameter of spherical small particles;

4) ignore friction of wall;

5) temperature is constant, without heat exchange with the outsid.

control equation

In view of internal flow field of sudden-expansion pipe is axisymmetric, and is vertical pipe flow, so the model is reduced to two-dimensional axisymmetric model in the cylindrical coordinate system. The solid-liquid phase of the control equation is as follows:

Liquid phase control equation

$$\frac{\partial}{\partial x}\left(\rho U\phi\right)+\frac{1}{r}\frac{\partial}{\partial r}\left(r\rho V\phi\right)=\frac{\partial}{\partial x}\left(\Gamma_\phi\frac{\partial\phi}{\partial x}\right)+\frac{1}{r}\frac{\partial}{\partial r}\left(r\Gamma_\phi\frac{\partial\phi}{\partial r}\right)+S_\phi+S_{\phi lp} \tag{1}$$

Where $\Phi = U, V, k, \varepsilon, m$ The values of Γ_ϕ, general diffusion coefficients，S_ϕ and $S_{\phi lp}$ the source terms, are given in table 1.

Table 1 liquid phase conservation equation

Conservation of :	ϕ	Γ_ϕ	S_ϕ	$S_{\phi lp}$
Mass	1	0	0	0
x-momentum	U	μ_e	$-\frac{\partial p}{\partial x}+\frac{\partial}{\partial x}\left(\mu_e\frac{\partial U}{\partial x}\right)+\frac{1}{r}\frac{\partial}{\partial r}\left(r\mu_e\frac{\partial V}{\partial x}\right)+\rho g$	$K_{pf}\left(U_P-U\right)$
r-momentum	V	μ_e	$-\frac{\partial p}{\partial r}+\frac{\partial}{\partial x}\left(\mu_e\frac{\partial U}{\partial r}\right)+\frac{1}{r}\frac{\partial}{\partial r}\left(r\mu_e\frac{\partial V}{\partial r}\right)-\frac{2\mu_e V}{r^2}$	$K_{pf}\left(V_P-V\right)$
Turbulent kinetic energy	k	μ_e/σ_k	$G_k-\rho\varepsilon$	G_P
Turbulent dissipation rate	ε	μ_e/σ_ε	$\frac{\varepsilon}{k}\left(C_{\varepsilon 1}G_k-C_{\varepsilon 2}\rho\varepsilon\right)$	$\varepsilon C_{\varepsilon 1}G_p/k$

solid phase control equation

$$\frac{\partial}{\partial x}\left(\rho_p U_p\phi_p\right)+\frac{1}{r}\frac{\partial}{\partial r}\left(r\rho_p V_p\phi_p\right)=\frac{\partial}{\partial x}\left(\Gamma_{\phi p}\frac{\partial\phi_p}{\partial x}\right)+\frac{1}{r}\frac{\partial}{\partial r}\left(r\Gamma_{\phi p}\frac{\partial\phi_p}{\partial r}\right)+S_{\phi p}+S_{\phi pl} \tag{2}$$

3

Copyright © 2010 by ASME

Table 2 solid phase conservation equation

Conservation of :	ϕ_p	$\Gamma_{\phi p}$	$S_{\phi p}$	$S_{\phi p l}$
Mass	1	v_p / σ_p	0	0
x -momentum	U_p	μ_p	$-\alpha_p \dfrac{\partial p}{\partial x} + \dfrac{\partial}{\partial x}\left(\mu_p \dfrac{\partial U_p}{\partial x}\right) + \dfrac{1}{r}\dfrac{\partial}{\partial r}\left(r\mu_p \dfrac{\partial V_p}{\partial x}\right)$ $+ \dfrac{\partial}{\partial x}\left(U_p \dfrac{v_p}{\sigma_p}\dfrac{\partial \rho_p}{\partial x}\right) + \dfrac{1}{r}\dfrac{\partial}{\partial r}\left(rU_p \dfrac{v_p}{\sigma_p}\dfrac{\partial \rho_p}{\partial r}\right)$ $\dfrac{\partial}{\partial x}\left(U_p \dfrac{v_p}{\sigma_p}\dfrac{\partial \rho_p}{\partial x}\right) + \dfrac{1}{r}\dfrac{\partial}{\partial r}\left(rV_p \dfrac{v_p}{\sigma_p}\dfrac{\partial \rho_p}{\partial x}\right) + \rho_p g$	$K_{fp}\left(U - U_P\right)$
r -momentum	V_p	μ_p	$-\alpha_p \dfrac{\partial p}{\partial r} + \dfrac{\partial}{\partial x}\left(\mu_p \dfrac{\partial U_p}{\partial r}\right) + \dfrac{1}{r}\dfrac{\partial}{\partial r}\left(r\mu_p \dfrac{\partial V_p}{\partial r}\right)$ $+ \dfrac{\partial}{\partial x}\left(V_p \dfrac{v_p}{\sigma_p}\dfrac{\partial \rho_p}{\partial x}\right) + \dfrac{1}{r}\dfrac{\partial}{\partial r}\left(rV_p \dfrac{v_p}{\sigma_p}\dfrac{\partial \rho_p}{\partial r}\right)$ $\dfrac{\partial}{\partial x}\left(U_p \dfrac{v_p}{\sigma_p}\dfrac{\partial \rho_p}{\partial r}\right) + \dfrac{1}{r}\dfrac{\partial}{\partial r}\left(rV_p \dfrac{v_p}{\sigma_p}\dfrac{\partial \rho_p}{\partial r}\right)$	$K_{fp}\left(V - V_P\right)$
Turbulent kinetic energy	k_p	μ_p / σ_p	$G_{pk} - \rho_p \varepsilon_p$	G_{pp}

$$G_k = \mu_t \left\{ 2\left[\left(\frac{\partial U}{\partial x}\right)^2 + \left(\frac{\partial V}{\partial r}\right)^2 + \left(\frac{V}{r}\right)^2 \right] + \left(\frac{\partial U}{\partial r} + \frac{\partial V}{\partial x}\right)^2 \right\} \quad (3)$$

$$G_p = K_{fp}\left[C_p^k \left(kk_p\right)^{1/2} - 2k \right] \quad (4)$$

$$G_{pk} = \rho_p v_p \left\{ 2\left[\left(\frac{\partial U_p}{\partial x}\right)^2 + \left(\frac{\partial V_p}{\partial r}\right)^2 + \left(\frac{V_p}{r}\right)^2 \right] + \left(\frac{\partial U_p}{\partial r} + \frac{\partial V_p}{\partial x}\right)^2 \right\} \quad (5)$$

$$G_{pp} = 2K_{fp}\left[C_p^k \left(kk_P\right)^{1/2} - k_p \right] \quad (6)$$

$$\varepsilon_p = -\frac{G_{pp}}{\rho_p} + \left[\frac{U - U_p}{\rho_p}\frac{v_p}{\sigma_p}\frac{\partial \rho_p}{\partial x} + \frac{V - V_p}{\rho_p}\frac{v_p}{\sigma_p}\frac{\partial \rho_p}{\partial r} \right] \quad (7)$$

$$\mu_e = \mu + \mu_t = \rho(v + v_t) = \rho v_e = \rho\left(v + C_\mu \frac{k^2}{\varepsilon} \right) \quad (8)$$

$$\mu_p = \rho_p v_p = \rho_p \left(C_{\mu p} \frac{k_p^2}{|\varepsilon_p|} \right) \quad (9)$$

Reference the parameter values in solid-liquid two-phase control equations is defined according to references (Zhou Lixing 2000; Zhou Lixing 1994; Ni Haoqing，Shen Yongming 1996), as shown in table 3.

Table 3 parameter in control equations

C_μ	$C_{\varepsilon 1}$	$C_{\varepsilon 2}$	σ_k	σ_ε	σ_p	C_p^k	$C_{\mu p}$
0.06	1.45	1.92	1.0	1.3	0.8	0.9	0.0085

4   Copyright © 2010 by ASME

EROSION MODEL

The effect of two phase flow on the erosion rate is single. The wearing tubing under throttle nozzle is analyzed as the simple, the results show that, the surface of the materials of tubing wear as the ploughing. This paper establishes the erosion model, based on the Finnie.I cutting wear erosion classical theory of plastic material. The established erosion model is shown in equation 10 and 11:

$$E = K m_p V_p^n f(\alpha) \qquad (10)$$

$$f(\alpha) = \begin{cases} \sin 2\alpha - 3\sin^2 \alpha & (\alpha \le \alpha_{max}) \\ \dfrac{\cos^2 \alpha}{3} & (\alpha \ge \alpha_{max}) \end{cases} \qquad (11)$$

Where, E is the erosion rate, $K = 0.03$ and $n = 2.4$, which are empirical constants determined according to the erosion experiment in this paper，m_p is particle flux, α is impact angle of particle，α_{max} is the impact angle as the erosion rate is maximum , V_p is the impact velocity of particle.

EROSION SIMULATION

Model simplification

Inlet length has a less effect on the internal fluid flow than outlet length, the computation model can to be considered is shown schematically in Figure 4. 2D axial symmetry model is built ,and the unit amount of grid is about 2×10^4.
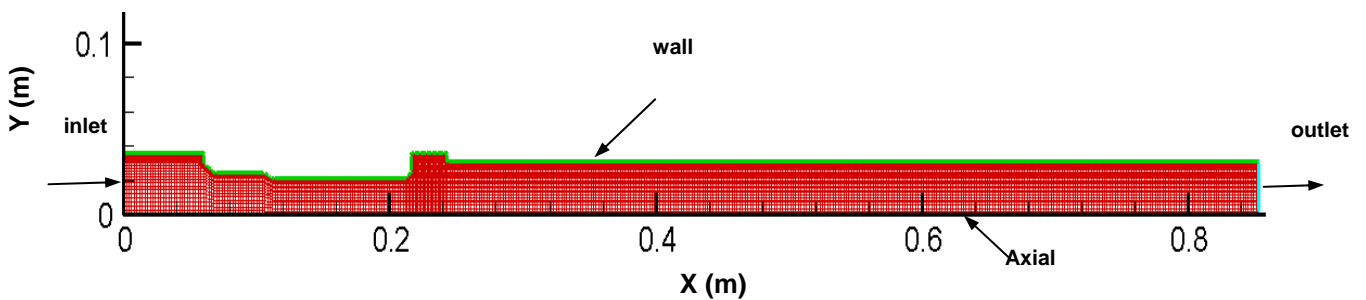

Figure 4 computation model and grid

Boundary

Liquid boundary
Inlet：
Velocity inlet, axial mean velocity , u_f ,radial velocity, $v_f = 0$, $k_f = 0.005 u_f^2$, $\varepsilon_f = \dfrac{500 C_\mu k_f^2}{u_f d_{inlet}}$;

outlet：$\dfrac{\partial \phi_f}{\partial x} = 0 (\phi_f = u_f, v_f, k_f, \varepsilon_f)$;

wall：no slip wall, standard wall function.

·Solid boundary
Inlet：
$$u_p = u_f, v_f = 0; \quad k_P = 0.0384 \, \mathrm{Re}_{d_{inlet}}^{-1/4} u_P^2 ;$$

The solid phase volume fraction $\alpha_p = 1 - \alpha_f$

Outlet：$\dfrac{\partial \phi_p}{\partial x} = 0 (\phi_p = u_p, v_p, k_p)$

Wall：The gradient of velocity of wall is zero, the exchange between the particles with the wall meet the zero-flux conditions.

Axis boundary：$v = 0 \quad \dfrac{\partial \phi_p}{\partial r} = 0 (\phi_p = u_p, k_p)$

Computation method and condition

The control equations are dispersed by the finite volume method. SIMPLE arithmetic is adopted to couple the pressure and velocity. The disperse format is the second up-wind. The density of sand particle is $1.72 \times 10^3 \mathrm{kg/m}^3$, its mean diameter is 5×10^{-5}m, viscosity coefficient of the fracture fluid is 100mPa/s, its density is $1.02 \times 10^3 \mathrm{kg/m}^3$, the volume fraction is 30％, the flow rate of inlet is 6m³/min.

CONCLUSION AND DISCUSSION

Flow streamlines

The velocity streamline at the sudden expansion cross section is shown in Figure 6, the direction of the arrow denotes the fluid flow direction. As shown in figure 6, the separation flow and reattachment occur at the sudden expansion cross section, there is the recirculation zone at the corner following sudden expansion. The fluid impacts internal surface of the tubing at the downstream of the straight tubing section. The velocity is high in the center of the tubing, and low in the separation and reattachment region.
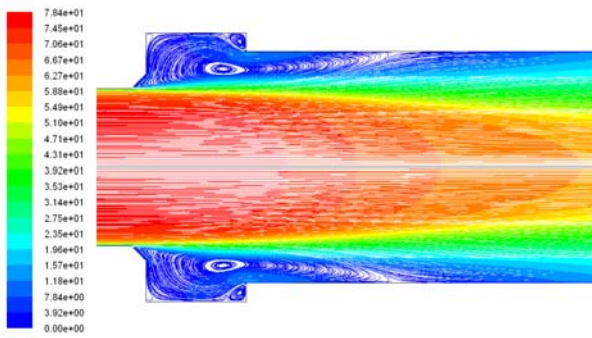
5

Copyright © 2010 by ASME
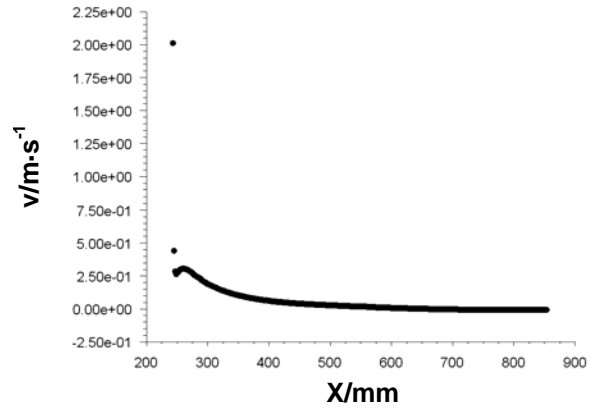
Figure 5 Velocity Streamline

Sand concentration profile

The volume fraction of particle is relatively stable at the centre of tubing, the sand particle distributes nonuniformly in the separation region. The concentration of sand particle is high outside of recirculation, the sand concentration at the centre of recirculation is low, and the sand particle flow downstream along the wall of tubing. After the reattachment point the concentration of sand particle near the wall in accord with the centre of the tubing.
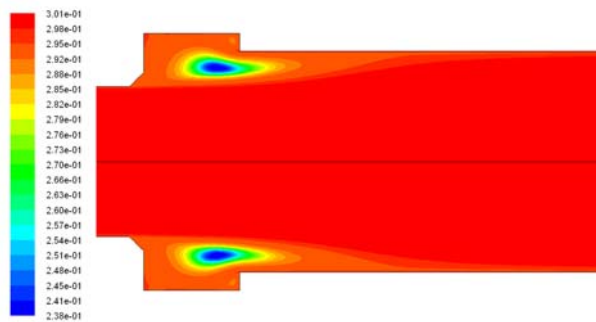
Figure 7 sand concentration

Velocity analysis

Figure 8 Mean axial particle velocity distribution

Figure 9 Mean radial particle velocity distribution

The mean axial and radial particle velocity distribution is shown in figure 8 and figure 9, the velocity value is from the corner of small constriction after the sudden expansion to the outlet. The mean axial velocity increases with increasing the x value near the wall, and decreases with increasing the x value at the centre. The mean radial velocity gradually decreases with increasing the x value.

Erosion analysis

The sudden expansion flow field, including flow separation recirculation and reattachment, and rates of erosion can be predicted for a wide range of system geometries. In addition, the velocities and angles of impact of suspended sand particles with the flow system walls can be determined for application to the calculation of the erosion rate. The impact angles and the velocity are shown in figure 10 and figure 11.
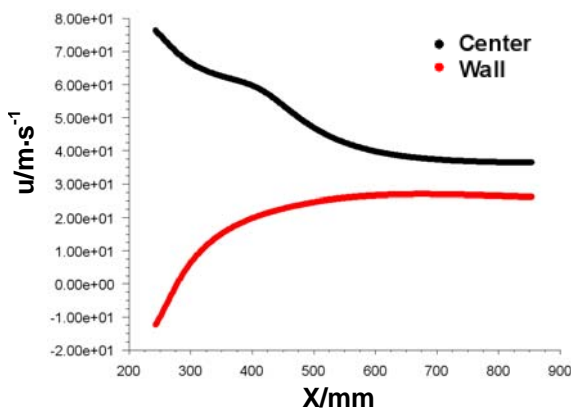

Figure 10 Mean impact angles

Figure 11 Mean impact velocity

6

Copyright © 2010 by ASME
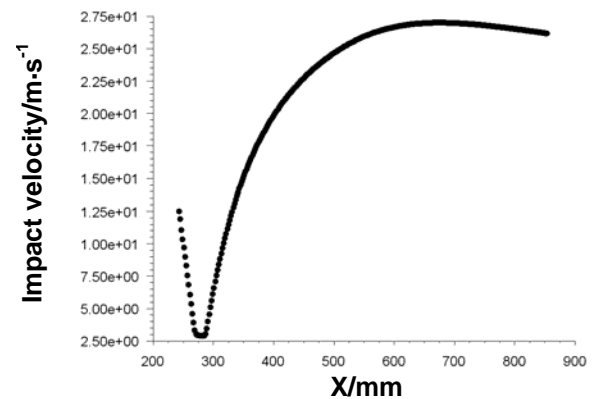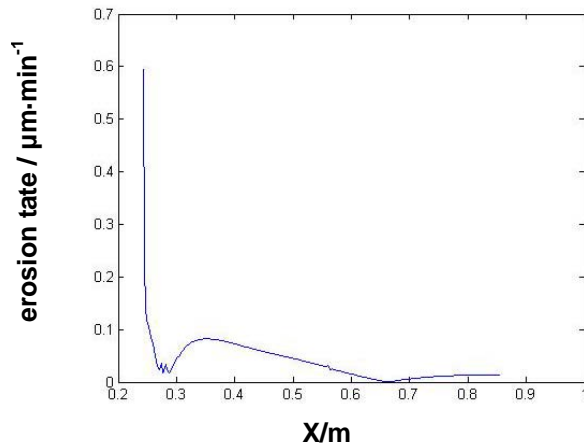
Figure 12 Erosion rates

The erosion model has been applied to the prediction of wear in fracturing sand slurries of fracture, the erosion rate is shown in figure 12. The erosion rate high values at the leading edge of small sudden constriction after expansion, and at the downstream the erosion rate rapidly decrease, at near the reattachment the erosion rate continue to increase, where the impact velocity and the impact angle is much higher. As expected, with increasing the x value, the erosion is low in the straight section.

CONCLUSION

Based on CFD, the Euler-Euler approach in conjunction with a k-ε turbulence model has been used to predict the motion of fracturing fluid and sand particle in sudden expansion, investigate the position of highly localised erosion in slurry tubing on fracturing used in deep gas wells. The streamline , sand concentration profile and velocity distribution were received. The erosion rate has been developed using the Finnie erosion model combining on the erosion experiment. The model was able to successfully predict the cause and position of the erosion, which agree well with the results of site fracturing operation, and can be used in the development of a new fracturing tubing design on highly flow rate fracture.

ACKNOWLEDGMENTS

REFERENCE

Lotz, E. Heitz, Werkst. Korros.34(1983):p. 454.

S. Nesic, J. Postlethwaite, Corrosion 47 (1991): p. 582.

J. Postlethwite, S. Nesic, G.. Adamopoulos, D.J. Bergstrom, "Predictive Models for Erosion-Corrosion Under Disturbed Flow Conditions," Proceedings of Advances in Corrosion and Protection, paper no.150, (Manchester, U.K.: UMIST, 1992).

Oliveira P J, Pinho F T. Pressure drop coefficient of laminar Newtonian flow in axisymmetric sudden expansions[J]. International Journal of Heat and Fluid Flow, 1997, 18:518-529

J. Postlethwaite, S. Nesic, G. Adamoroulos and D.J.Bergstrom. Predictive models for erosion-corrosion under disturbed flow conditions, Corrosion Science, Vol. 35, Nos1-4, pp. 627-633, 1993.

Zhou Lixing. Multi-phase turbulent reaction fluid dynamics [M]. Beijing: National Defense Industry Press，2000.

Zhou Lixing. Turbulent two-phase flow and combustion theory and numerical simulation [M]. Beijing: Science Press，1994.

Ni Haoqing，Shen Yongming. Engineering turbulent flow, heat transfer and mass transfer numerical simulation [M].Beijing: China Water Conservancy and Hydropower Press，1996

NOMENCLATURE

x axial coordinate，m

r radial coordinate，m

ρ density of the liquid phase，kg m^{-3}

U ,V components of liquid phase mean velocity vector, m s^{-1}

U_p ,V_p components of solid phase mean velocity vector, m s^{-1}

g acceleration of gravity

p pressure, N m^{-2}

ν kinematic viscosity of liquid phase, m^{2}s^{-1}

ν_t turbulent kinematic eddy viscosity coefficient

α_p volume fraction of the solid phase

ν_p kinematic viscosity of solid phase, m^{2}s^{-1}

K_{fp} , K_{pf} The fluid-solid exchange coefficient , $K_{fp} = K_{pf}$

k turbulent kinetic energy of the liquid phase

ε dissipation rate of the liquid phase

k_p turbulent kinetic energy of the solid phase

ε_p dissipation rate of the solid phase

ν_e effective kinematic viscosity coefficient

d_p diameter of the solid phase, m

ρ_p density of the solid phase, kg m^{-3}

E erosion rate, μm·min^{-1}